Effective operator for $d-d$ transitions in nonresonant inelastic x-ray scattering

Michel van Veenendaal[1,2,*] and M. W. Haverkort[3,4]

[1]*Department. of Physics, Northern Illinois University, De Kalb, Illinois 60115, USA*
[2]*Advanced Photon Source, Argonne National Laboratory, 9700 South Cass Avenue, Argonne, Illinois 60439, USA*
[3]*II. Physikalisches Institut, Universität zu Köln, Zülpicher Str. 77, D-50937, Köln, Germany*
[4]*Max-Planck-Institut für Festkörperforschung, D-70569, Stuttgart, Germany*

Recent experiments by Larson *et al.* [Phys. Rev. Lett. **99**, 026401 (2007)] demonstrate the feasibility of measuring local $d-d$ excitations using nonresonant inelastic x-ray scattering (IXS). We establish a general framework for the interpretation where the $d-d$ transitions created in the scattering process are expressed in effective one-particle operators that follow a simple selection rule. The different operators can be selectively probed by employing their different dependence on the direction and magnitude of the transferred momentum. We use the operators to explain the presence of nodal directions and the nonresonant IXS in specific directions and planes. We demonstrate how nonresonant IXS can be used to extract valuable ground state information for orbiton excitations in manganite.

I. INTRODUCTION

Transition-metal compounds display a wide variety of exciting phenomena such as high-T_c superconductivity, colossal magnetoresistance, and metal-insulator transitions resulting from the strong interplay between the charge, spin, and orbital degrees of freedom. Knowledge of the electronic and magnetic structure can be obtained by a variety of spectroscopic techniques such as optical spectroscopy, photoemission, x-ray absorption. A general understanding of spectroscopy and its uses has always been a crucial aspect in the advancement of condensed-matter physics. Recently, inelastic x-ray scattering (IXS), both on and off resonance, has attracted considerable attention. Resonant inelastic x-ray scattering (RIXS) (Ref. 1) is a second-order process dominated by $\mathbf{p} \cdot \mathbf{A}$, where $\mathbf{p}$ is the momentum and $\mathbf{A}$ the vector potential. The incoming x ray excites an electron from a deep-lying core state into the valence shell, and one measures the radiative decay of the core hole. For RIXS at the transition-metal L and M edges, the dipole transitions create $d-d$ excitations that include spin-flips due to the strong intermediate-state spin-orbit coupling.[2,3] The transitions can be described with an effective operator approach[3] in the fast-collision approximation. RIXS at the K edge, where excitations are predominantly shake-up processes by the strong $1s$ core potential,[4] can be related in certain limits to the dynamic structure factor $S_{\mathbf{q}}(\omega)$ (Ref. 5).

Nonresonant IXS, on the other hand, involves the interaction

$$\frac{e^2}{2m}\mathbf{A}^2 = \frac{e^2}{2m}\mathbf{e}' \cdot \mathbf{e}\, e^{i\mathbf{q} \cdot \mathbf{r}}, \tag{1}$$

with $\mathbf{q} = \mathbf{k} - \mathbf{k}'$ where $\mathbf{e}/\mathbf{e}'$ and $\mathbf{k}/\mathbf{k}'$ are the polarization and wave vectors of the incoming/outgoing x rays, respectively. The interaction due to the A^2 term is in principle weak. However, the successful experiments by Larson *et al.*[6] demonstrated the feasibility of measuring local $d-d$ excitations, and comparison of the radial matrix elements indicate that these transitions can in principle also be observed in other transition-metal and rare-earth compounds. The appealing feature of nonresonant IXS is that the cross section is proportional to the dynamic structure factor: $d^2\sigma/d\Omega d\omega \sim S_{\mathbf{q}}(\omega)$, which through the fluctuation-dissipation theorem is connected to the imaginary part of the density response function,

$$\chi_{\mathbf{q}}(\omega) = \langle g | \rho_{\mathbf{q}} \frac{1}{\omega + E_g - H + i0^+} \rho_{-\mathbf{q}} | g \rangle, \tag{2}$$

with E_g the ground state energy and where the Hamiltonian H, for transition-metal compounds, includes strong many-body interactions; $\rho_{\mathbf{q}}$ is the density operator

$$\rho_{\mathbf{q}} = \sum_{\mathbf{k} n n' \sigma} \langle \psi_{\mathbf{k}+\mathbf{q},n'\sigma} | e^{i\mathbf{q} \cdot \mathbf{r}} | \psi_{\mathbf{k}n\sigma} \rangle c^{\dagger}_{\mathbf{k}+\mathbf{q},n'\sigma} c_{\mathbf{k}n\sigma}, \tag{3}$$

where $c^{\dagger}_{\mathbf{k}n\sigma}$ creates an electron in a state $\psi_{\mathbf{k}n\sigma}$ where n is the band index and $\sigma = \uparrow, \downarrow$. Without matrix elements $\rho_{\mathbf{q}}$ becomes equivalent to the charge density operator $\rho_{\mathbf{q}} = \sum_{\mathbf{k}\sigma} c^{\dagger}_{\mathbf{k}+\mathbf{q},\sigma} c_{\mathbf{k}\sigma}$. However, matrix elements play a crucial role in the understanding of the inelastic scattering. Using Wannier functions, we can rewrite the matrix element in terms of scattering from an atom at site $\mathbf{R}_0$ to a site $\mathbf{R}$,

$$\langle \psi_{\mathbf{k}+\mathbf{q},n'\sigma} | e^{i\mathbf{q} \cdot \mathbf{r}} | \psi_{\mathbf{k}n\sigma} \rangle = \sum_{\mathbf{R}} e^{i\mathbf{q} \cdot \mathbf{R}} \langle \phi_{\mathbf{R}\alpha'\sigma} | e^{i\mathbf{q} \cdot \mathbf{r}} | \phi_{\mathbf{R}_0\alpha\sigma} \rangle, \tag{4}$$

where $\phi_{\mathbf{R}\alpha\sigma}$ is a localized Wannier orbital of type α at site $\mathbf{R}$. The operator $\rho_{\mathbf{q}}$ can create charge-transfer transitions (with $\mathbf{R} \neq \mathbf{R}_0$), plasmon excitations,[7–9] and dipolar and higher-order transitions from core to valence states (where $\mathbf{R} = \mathbf{R}_0$).[10–13] Recently, it was demonstrated[6] that it is also possible to measure dipolar forbidden $d-d$ transitions. By tuning the transferred momentum,[6,14] one is able to maximize the intensity for local transitions ($\mathbf{R}_i = \mathbf{R}_j$) within the $3d$ shell, for which the matrix element is

$$\langle \phi_{\mathbf{k}+\mathbf{q},n'} | e^{i\mathbf{q} \cdot \mathbf{r}} | \phi_{\mathbf{k}n} \rangle \cong \langle \phi_{3d,\alpha'} | e^{i\mathbf{q} \cdot \mathbf{r}} | \phi_{3d,\alpha} \rangle, \tag{5}$$

where α denotes the different $3d$ orbitals. This approximation assumes reasonably well "localized" Warnier orbitals.

These sharp dipole-forbidden transitions were first observed by Larson *et al.*[6] for large q in NiO and CoO. The use of large wave vectors would allow a resolution of 30 meV or less, making nonresonant IXS a promising tool to study local crystal field and orbiton excitations. It could be used, for example, to study the Jahn–Teller distortions in manganites and the nature of the small crystal field distortions in early transition-metal oxides. Although the angular dependence in NiO and CoO has been analyzed with density-functional theory[6] and small-cluster calculations,[14] the detailed nature of the angular dependence and how to use it is not well understood. In this paper, we express $\rho_{\mathbf{q}}$ as an effective operator, derive the selection rules governing the local $d-d$ transitions, and give explicit angular dependencies. We provide an explanation for the remarkable intensity variations in certain directions. The derivation for the angular distribution of the intensities is partially based on symmetry rules and should therefore be very generally valid. We show how IXS can be used to extract detailed ground-state information by treating the IXS from orbitons (excitonic orbital excitations not involving the Hubbard U) in manganites.

II. EFFECTIVE OPERATORS AND SELECTION RULES

For local $d-d$ transitions, it is convenient to express the $3d$ Wannier functions $\phi_{\mathbf{R}_0 m} = R_{3d}(r) Z_m^{(2)}(\hat{\mathbf{r}})$, with $r = |\mathbf{r}|$ and $\hat{\mathbf{r}} = \mathbf{r}/r$, in terms of a radial function $R_{3d}(r)$ and a real angular part

$$Z_m^{(l)}(\hat{\mathbf{r}}) = N_m \sqrt{\frac{4\pi}{2l+1}} [Y_{-\bar{m}}^{(l)}(\hat{\mathbf{r}}) + s_m Y_{\bar{m}}^{(l)}(\hat{\mathbf{r}})], \qquad (6)$$

where $\bar{m} = |m|$, $N_m = 1, \frac{1}{\sqrt{2}} i^{(1-\operatorname{sgn} m)/2}$, and $s_m = 0, (-1)^m \operatorname{sgn}(m)$ for $m = 0$ and $\bar{m} > 0$, respectively; $Y_m^{(l)}(\hat{\mathbf{r}})$ is a spherical harmonic. The functions $Z_m^{(l)}(\hat{\mathbf{r}})$ are known as tesseral harmonics and convenient when dealing with transition-metal compounds since the values $m = -2, -1, 0, 1, 2$ correspond to the $3d$ orbitals $d_{xy}, d_{yz}, d_{3z^2-r^2}, d_{xz}, d_{x^2-y^2}$, respectively (see Table I). We can expand the exponent in Eq. (1) in terms of Bessel functions and tesseral harmonics,

$$e^{i\mathbf{q}\cdot\mathbf{r}} = \sum_{LM} (2L+1) i^L j_L(qr) Z_M^{(L)}(\hat{\mathbf{q}}) Z_M^{(L)}(\hat{\mathbf{r}}), \qquad (7)$$

where $M = -L, -L+1, \cdots, L$, and j_L is a Bessel function of order L. Spherical-tensor algebra gives an effective transition operator

$$\rho_{\mathbf{q}} = \sum_L A_L(q) \sum_M Z_M^{(L)}(\hat{\mathbf{q}}) w_M^L, \qquad (8)$$

consisting of a one-particle transition operator w_M^L probed by $\mathbf{q}$ through a reduced matrix element $A_L(q)$ and an angular dependence $Z_M^{(L)}(\hat{\mathbf{q}})$. Of the summation over L only the values 0 (monopolar), 2 (quadrupolar), and 4 (hexadecapolar) remain. The factor

$$A_L(q) = i^L (2L+1) C_{20,L0}^{20} C_{22,L0}^{22} P_L, \qquad (9)$$

where $C_{l_1 m_1, l_2 m_2}^{l_3 m_3}$ are Clebsch–Gordan coefficients, and $P_L(q) = \int dr\, r^2 R_{3d}(r) j_L(qr) R_{3d}(r)$ is the reduced matrix ele-

TABLE I. The angular dependence $U_{mm'}(\hat{\mathbf{q}}) = \langle m'|\rho_{\mathbf{q}}|m\rangle$ of the scattering between orbitals m and m'. The real $3d$ orbitals are $Z_m^{(2)} = \sqrt{3}\hat{x}\hat{y}, \sqrt{3}\hat{y}\hat{z}, \frac{3}{2}\hat{z}^2 - \frac{1}{2}, \sqrt{3}\hat{x}\hat{z}$, and $\frac{1}{2}\sqrt{3}(\hat{x}^2 - \hat{y}^2)$ for $m = -2, -1, 0, 1, 2$; $\hat{\mathbf{q}} = (\hat{x}, \hat{y}, \hat{z}) = (\sin\theta\cos\varphi, \sin\theta\sin\varphi, \cos\theta)$, in conventional spherical coordinates θ and φ. For off-diagonal matrix elements ($m \neq m'$) for t_{2g} ($m = \pm 1, -2$) orbitals, m'' denotes the t_{2g} orbital for which $m'' \neq m, m'$. The coordinate $\hat{r}_m = \hat{y}, \hat{x}, \hat{z}$ for $m = 1, -1, \pm 2$.

m	m'	$U_{mm'}(\hat{\mathbf{q}})$
$m' = m$:		
0		$A_2(-\frac{3}{2}\hat{z}^2 + \frac{1}{2}) + \frac{3}{4}A_4(35\hat{z}^4 - 30\hat{z}^2 + 3)$
$\neq 0$		$A_2(\frac{3}{2}\hat{r}_m^2 - \frac{1}{2}) + A_4(5\hat{r}_m^2 - 4 + \frac{35}{3}[Z_m^{(2)}]^2)$
$m' \neq m$:		
$\pm 1, -2$	$\pm 1, -2$	$[-\frac{\sqrt{3}}{2}A_2 + \frac{5}{3}\sqrt{3}A_4(7\hat{r}_{m''}^2 - 1)]Z_{m''}^{(2)}$
± 1	0	$[-\frac{1}{2}A_2 + \frac{5}{2}A_4(7\hat{z}^2 - 3)]Z_{\pm 1}^{(2)}$
± 1	2	$[\mp\frac{\sqrt{3}}{2}A_2 + \frac{5}{6}\sqrt{3}A_4\{7(\hat{x}^2 - \hat{y}^2) \pm 2\}]Z_{\pm 1}^{(2)}$
± 2	0	$[A_2 + \frac{5}{2}A_4(7\hat{z}^2 - 1)]Z_{\pm 2}^{(2)}$
2	-2	$\frac{35}{2}A_4 \hat{x}\hat{y}(\hat{x}^2 - \hat{y}^2)$

ment of the Bessel function. For brevity, we implicitly assume the dependence on q and $\hat{\mathbf{q}}$ in the remainder. $A_L = P_0, \frac{10}{7}P_2, \frac{3}{7}P_4$, for $L = 0, 2$, and 4, respectively. In second quantization, the transition operator is

$$w_M^L = \sum_{m\sigma} \sum_{\substack{m' = m_{\pm} \\ m_- \neq m_+}} a_{mm'}^{LM} d_{m'\sigma}^{\dagger} d_{m\sigma}, \qquad (10)$$

where $d_{m\sigma}^{\dagger}$ creates an electron with spin $\sigma = \uparrow, \downarrow$ in the $3d$ orbital with index m. The transition probability is

$$a_{mm_{\pm}}^{LM} = \delta_{m_{\pm}, \operatorname{sgn}(mM)|\bar{m} \pm \bar{M}|} \frac{N_{m_{\pm}}^* N_m N_M P_{mM}^{\pm}}{C_{20,l0}^{20}} C_{2\bar{m},l,\pm\bar{M}}^{2,\bar{m} \pm \bar{M}}$$

with $P_{mM}^- = 2s_M, 2s_m$ for $\bar{m} \pm \bar{M} \geq 0$ and $\bar{m} \pm \bar{M} \leq 0$, respectively, and $P_{mM}^+ = 2 - \delta_{m,0}\delta_{M,0}$.

For the monopole term ($L = 0$), the scattering is elastic and isotropic, since

$$w_0^0 = n_e = \sum_{m\sigma} d_{m\sigma}^{\dagger} d_{m\sigma}, \qquad (11)$$

and $Z_0^{(0)}(\hat{\mathbf{q}}) = 1$.

For inelastic scattering in transition-metal systems, the coefficient contains the simple selection rule

$$m' = \operatorname{sgn}(mM)|m \pm M|, \qquad (12)$$

under the conditions that $|m'| \leq 2$ and $\operatorname{sgn}(mM) = 1$ for $m' = 0$. This selection rule helps us to obtain an understanding of nonresonant IXS. As an example, let us consider a Cu^{2+} ion in D_{4h} symmetry for quadrupolar ($L = 2$) scattering. The ground state is $|\underline{d}_{x^2-y^2}\rangle$ ($m = 2$), where the underline indicates holes. When measuring along the [001] direction, the only nonzero angular term is $Z_0^{(2)} = \frac{3}{2}\hat{z}^2 - \frac{1}{2}$ ($m = 0$), where we use $\hat{\mathbf{q}} = (\hat{x}, \hat{y}, \hat{z}) = (\sin\theta\cos\varphi, \sin\theta\sin\varphi, \cos\theta)$ in conventional spherical coordinates θ and φ. There is no inelastic scattering since the relevant transition operator w_0^2 only contributes to the elastic intensity ($m = 2 \rightarrow 2$). When measuring with $\mathbf{q}$ in

the xy plane, $Z_M^{(L)}$ is zero for odd M. For even M, w_0^2 gives elastic scattering; w_{-2}^2 does not contribute since transitions to $m' = -0, -4$ are forbidden since $\text{sgn}(mM) = 1$ is not satisfied for $m' = 0$ and $|m'| \leq 2$ for $3d$ electrons. The only inelastic scattering is due to w_2^2, giving $\underline{d}_{x^2-y^2} \rightarrow \underline{d}_{3z^2-r^2}$ (or $m = 2 \rightarrow 0$) with a $Z_2^{(2)} = \frac{\sqrt{3}}{2}(\hat{x}^2 - \hat{y}^2)$ angular dependence. In addition, we can easily see that transitions $\underline{d}_{x^2-y^2} \rightarrow \underline{d}_{xy}$ ($m = 2 \rightarrow -2$) are possible for operators with symmetry -0 and -4 using the inverse relationship $M = \text{sgn}(mm')|m \pm m'|$. However, -0 does not satisfy the condition that $\text{sgn}(mm') = 1$ for $M = 0$ and is therefore not allowed. The transition $\underline{d}_{x^2-y^2} \rightarrow \underline{d}_{xy}$ is therefore hexadecapolar ($L = 4$, $M = -4$).

Although all the off-diagonal terms for the quadrupolar scattering are determined by a single M, often two different M values interfere. It is therefore convenient to define a total angular dependence between two $3d$ orbitals by $U_{mm'}(\hat{\mathbf{q}}) = \langle m' | \rho_{\mathbf{q}} | m \rangle$, which are given in Table I. We now demonstrate how the selection rules and symmetry can help in extracting valuable ground-state information.

III. IXS IN HIGH-SYMMETRY DIRECTIONS

One of the striking features of nonresonant inelastic x-ray scattering in NiO is the presence of a [001] nodal direction absent in CoO. Larson *et al.*[6] ascribed this to a "**q**-selection rule" associated with the nearly cubic point group symmetry of NiO. The absence of inelastic scattering, $\langle f | \rho_{\mathbf{q}} | g \rangle = 0$, implies $\rho_{\mathbf{q}} | g \rangle = \text{const} | g \rangle$. This occurs when H and $\rho_{\mathbf{q}}$ commute, $[H, \rho_{\mathbf{q}}] = 0$. In general, this rarely happens, but $\rho_{\mathbf{q}}$ can commute with parts of the Hamiltonian, which then might give rise to nodal directions for all excited states if $\rho_{\mathbf{q}} | g \rangle = \text{const} | g \rangle$ and otherwise gives a nodal direction for the excited states for which $\langle f | \rho_{\mathbf{q}} = \langle f | \text{const}$. Below we will first discuss the commutation relations between $\rho_{\mathbf{q}}$ and the crystal-field operator, and then those with the Coulomb interaction. For $\mathbf{q} = q\hat{\mathbf{z}}$, the only nonzero angular dependence $Z_0^{(L)}$ selects the operators w_0^L. This gives a density operator diagonal in m,

$$\rho_{q\hat{\mathbf{z}}} = \sum_{m\sigma} Q_m d_{m\sigma}^\dagger d_{m\sigma} \tag{13}$$

with

$$Q_m = A_2\left(\frac{1}{2}m^2 - 1\right) + A_4\left(\frac{35}{12}m^4 - \frac{155}{12}m^2 + 6\right). \tag{14}$$

In several common crystal-fields, such as O_h and D_{4h}, m is a good quantum number and therefore $\rho_{\mathbf{q}}(\hat{\mathbf{z}})$ commutes with the crystal-field operator. Along [100], $\rho_{q\hat{\mathbf{x}}}$ is no longer diagonal but, since it is a unitary transformation over $90°$ of $\rho_{q\hat{\mathbf{z}}}$, it still only contains $e \rightarrow e$ and $t_2 \rightarrow t_2$, but no $e \rightarrow t_2$ scattering. Eigenstates of the octahedral crystal field therefore scatter among themselves. Thus, for a system with a O_h or D_{4h} symmetry a nodal direction can occur when $\mathbf{q} \| C_4$, where C_4 is a fourfold symmetry axis. Since in general $\rho_{\mathbf{q}}$ does not commute with the Coulomb interaction, the eigenstate of the crystal field should also be an eigenstate of the Coulomb interaction. This occurs for high-spin $3d^n$ configurations, except $3d^2$ and $3d^7$. For example, the ground state for a Ni^{2+}

ion (in the absence of spin-orbit coupling) is $\underline{d}_{3z^2-r^2\uparrow}\underline{d}_{x^2-y^2\uparrow}$. This is an eigenstate of the crystal field, the Coulomb interaction, and $\rho_{q\hat{\mathbf{z}}}$. Therefore, no inelastic scattering occurs along all six C_4 axes. On the other hand, for Co^{2+}, the ground state is given by $| g \rangle = \alpha | \underline{d}_{t_2\uparrow} d_{e\uparrow}^2 (^4T_1) \rangle + \beta | \underline{d}_{t_2\uparrow}^2 d_{e\uparrow} (^4T_1) \rangle$, where the mixing occurs due the Coulomb interaction. This is not an eigenstate of the octahedral crystal field and the operators $\rho_{q\hat{\mathbf{z}}}$, and inelastic scattering in the [001] direction therefore occurs into the excited multiplet

$$| f \rangle = \beta | \underline{d}_{t_2\uparrow} d_{e\uparrow}^2 (^4T_1) \rangle - \alpha | \underline{d}_{t_2\uparrow}^2 d_{e\uparrow} (^4T_1) \rangle, \tag{15}$$

which is about 2.4 eV higher in energy.[14] Also, deviations from a $t_2 e^2$ ground state due to band effects and a lowering of the crystal field[1] give rise to inelastic scattering. Spin-orbit coupling can also remove a nodal direction, but its effect is small except when the spin-orbit coupling lifts a degeneracy. Finally, the conditions for nodal directions above are generally not satisfied for low- and intermediate-spin ground states.

IV. ORBITON EXCITATIONS IN MANGANITES

Orbital physics plays an important role in manganites, which have been extensively studied for their magnetoresistive behavior.[15] $LaMnO_3$ is known to have an alternating $d_{3x^2-r^2}/d_{3y^2-r^2}$ orbital ordering, and half-filled systems often display the *CE* type structure with charge and orbital order occurring in an unconventional zigzag magnetic structure. However, others have contested this ionic picture stating that the ground state is more complex. For example, for $La_{0.5}Sr_{1.5}MnO_4$, it was claimed, based on x-ray magnetic linear dichroism experiments,[16] that a significant out-of-plane character was mixed in, giving an orbital ordering close to $d_{x^2-z^2}/d_{y^2-z^2}$. We demonstrate the extreme sensitivity of the angular dependence of nonresonant IXS on the detailed nature of the ground state. The ground state for Mn^{3+} is given by a $d_{t_2\uparrow}^3 d_{e\uparrow}$ configuration. Degenerate e orbitals $d_{3z^2-r^2}$ ($m = 0$) and $d_{x^2-y^2}$ ($m = 2$) are sensitive to distortions leading to lowest states given by $| e_\pm \rangle = \pm \alpha | 2 \rangle + \beta | 0 \rangle$, with $\alpha^2 + \beta^2 = 1$. The phases account for the different orientations of the orbitals due to orbital ordering often found in manganites. With nonresonant IXS, one can make excitations into the empty state $| e_\pm^* \rangle = \alpha | 0 \rangle \mp \beta | 2 \rangle$ by exciting an electron from the e ($d_{t_2\uparrow}^3 d_{e_\pm\uparrow} \rightarrow d_{t_2\uparrow}^3 d_{e_\pm^*\uparrow}$) or t_2 states ($d_{t_2\uparrow}^3 d_{e_\pm\uparrow} \rightarrow d_{t_2\uparrow}^2 d_{e_\pm\uparrow} d_{e_\pm^*\uparrow}$). For the former, the inelastic intensity summed over both $e_\pm$ orientations is

$$\sum_{p=\pm} |\langle e_p^* | \rho_{\mathbf{q}} | e_p \rangle|^2 = 2\alpha^2\beta^2(U_{00} - U_{22})^2 + 2(\alpha^2 - \beta^2)^2 U_{20}^2$$

(see also Table I). Figure 1 shows the angular dependencies for different ground-state orbitals given by α^2, see Fig. 1(a). Let us first look at the quadrupolar region ($A_2 = 1$, $A_4 = 0$), see Fig. 1(b). The angular dependence can be rewritten as $8\alpha^2\beta^2(\frac{3}{2}\hat{z}^2 - \frac{1}{2})^2 + 2(\alpha^2 - \beta^2)^2\frac{3}{4}(\hat{x}^2 - \hat{y}^2)^2$ and can be straightforwardly used to extract the value of α. A typical experiment is comparable to those of Larson *et al.*[6] One fixes the magnitude of the transferred momentum and changes its angle. For example, the intensity when rotating the angle
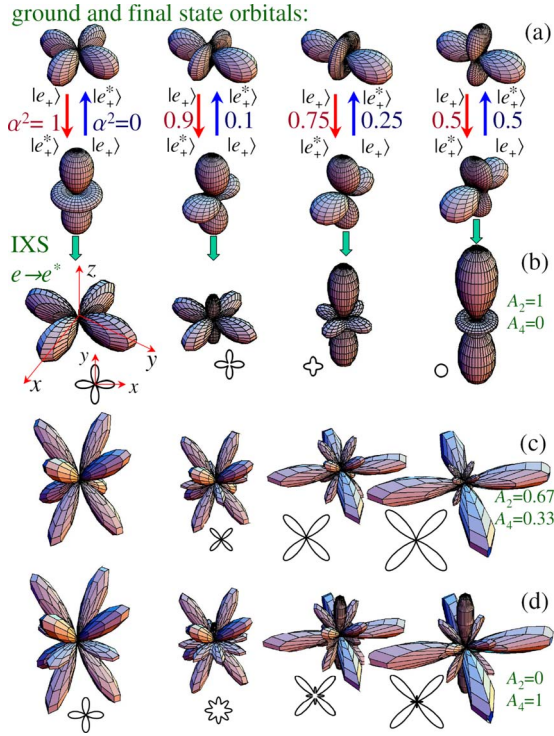
ground and final state orbitals:

FIG. 1. (Color online) Inelastic scattering from $e \rightarrow e^*$ in the manganites. (a) The top part shows the lowest e orbitals for $|e_+\rangle = \alpha|2\rangle + \beta|0\rangle$ for $\alpha^2 = 1$, 0.9, 0.75, and 0.5. Excitations are made into the orbital $|e_+^*\rangle = \alpha|0\rangle - \beta|2\rangle$. The angular dependence for $\alpha^2 = 0, 0.1, 0.25, 0.5$ is the same as those for $1 - \alpha^2$. The inversion of the relative energy positions of the orbitals does not affect the non-resonant IXS, which is proportional to $|\langle e_\pm^*|\rho_\mathbf{q}|e_\pm\rangle|^2$. (b) The angular distribution of the nonresonant IXS intensity in the quadrupolar region ($A_2 = 1$ and $A_4 = 1 - A_2 = 0$). The intensity in a certain direction is proportional to the distance to the origin. The insets show the intensity in the xy plane. The intensities give the sum over both orientations of the $e_\pm$ orbitals; (c) same as (b) for $A_2 = 0.67$; (d) idem for $A_2 = 0$.

from the [001] to the [100] direction depends strikingly on α. For $\alpha = 1$, which corresponds to an electron in the $x^2 - y^2$ orbital, the IXS intensity is predominantly along the x and y directions. For $\alpha = \frac{1}{\sqrt{2}}$, the angular intensity is predominantly along the z direction. However, when the hexadecapolar contribution increases, such an interpretation is less straightforward [see Fig. 1(c) and 1(d)]. However, simplifications occur when looking in specific directions or planes. First, note that the [001] direction is only nodal when $|e_+\rangle = |2\rangle$ or $|0\rangle$, which are good eigenfunctions of $\rho_{q\hat{z}}$. However, more quantitative information can be obtained by comparing the intensities along [001] and [100] or [010]. The $e \rightarrow e$ scattering along [001] depends on the parameters $Q_0 = -A_2 + 6A_4$ and $Q_2 = A_2 + A_4$ [see Eqs. (13) and (14)]. However, for inelastic scattering, we can remove one of those parameters by rewriting the scattering operator as $\rho_{q\hat{z}} = Q_0 n_e + \sum_{m \neq 0, \sigma} (Q_m - Q_0) d^\dagger_{m\sigma} d_{m\sigma}$. The number operator n_e only gives elastic scattering, so effectively the $e \rightarrow e$ scattering only depends on $Q_{20} = Q_2 - Q_0 = 2A_2 - 5A_4$. Along [100], $\rho_{q\hat{x}}$ only contains $e \rightarrow e$ and $t_2 \rightarrow t_2$, but no $e \rightarrow t_2$ scattering. The $e \rightarrow e$ scattering again only depends on Q_{20}. A straightforward calculation gives for the
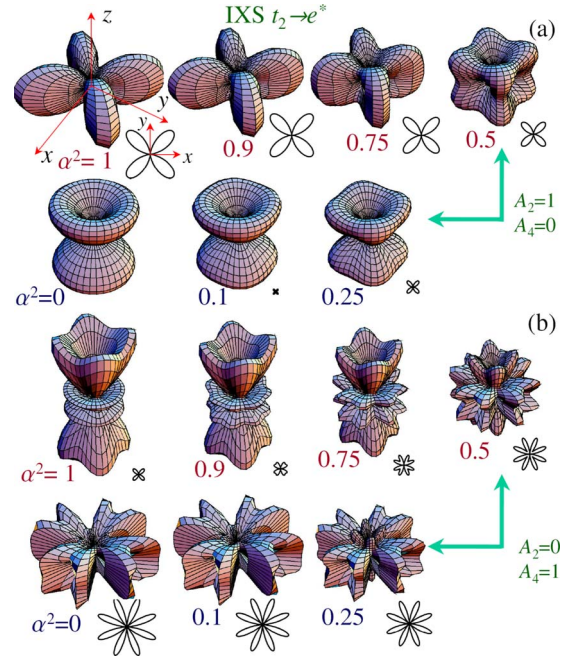

FIG. 2. (Color online) Nonresonant inelastic scattering for the manganites with an electron in the $|e\rangle$ states as in Fig. 1(a), but now for scattering $t_2 \rightarrow e^*$ for $\alpha^2 = 1$, 0.9, 0.75, 0.5, 0.25, 0.1, and 0. Note that now α^2 and $1 - \alpha^2$ are inequivalent. (a) Nonresonant IXS in the quadrupolar region ($A_2 = 1$ and $A_4 = 0$); (b) idem in the hexadecapolar region ($A_2 = 0$ and $A_4 = 1$). The insets show the scattering intensity in the xy plane.

ratio of the nonresonant scattering intensities in the [001] and [100] direction

$$I_{[001]}/I_{[100]} = 16\alpha^2\beta^2/(3 - 8\alpha^2\beta^2). \qquad (16)$$

Note that, since $\beta^2 = 1 - \alpha^2$, this ratio is independent of the reduced matrix elements and can be used to extract directly the nature of the Jahn–Teller distorted state. From the factor $Q_{20} = 2A_2 - 5A_4$, one also sees a destructive interference independent of α between quadrupolar and hexadecapolar terms in the x, y, and z directions, which is clearly visible in Fig. 1(c), where the intensity in those directions are almost zero. A clear feature that displays the change in ground state as a function of α^2 is the direction of the dominant lobes in the xy plane [see insets in Fig. 1(b)–1(d)]. Again, this can be used to obtain information on ground-state properties. The intensity in the x or y direction $\frac{1}{8}Q_{20}^2(3 - 8\alpha^2\beta^2)$ decreases with increased mixing of the $x^2 - y^2$ and $3z^2 - r^2$ orbitals, whereas along the [110] directions, the intensity $2\alpha^2\beta^2(A_2 + \frac{25}{4}A_4)^2$ increases.

The measurement of the $e \rightarrow e^*$ orbiton excitation has the great advantage that the energy loss can be directly related to the energy for an orbiton excitation. Since this energy is of the order of 0.3–1.5 eV, this feature might in practice be difficult to distinguish from the elastic line. However, valuable information can still be obtained from the study of the $t_2 \rightarrow e^*$ excitation, where an electron from the t^3_{2g} spin is excited into the empty e^* orbital. This excitation is at higher energy loss due to the crystal-field splitting between e and t_2,

which is of the order of 2–2.5 eV. The angular dependencies are shown in Fig. 2. First, note that the spectra for α^2 and $1-\alpha^2$ are no longer equivalent. Second, the x, y, and z directions are all nodal since no $t_2 \rightarrow e$ scattering occurs. Simplifications also occur in the xy plane. Scattering from $|0\rangle \rightarrow |\pm 1\rangle$, $|-2\rangle$ requires $M = \pm 1, -2$ and $|2\rangle \rightarrow |\pm 1\rangle$, $|-2\rangle$ requires $M = \pm 1 (\pm 3)$ and (-4), respectively (M values in parentheses give pure hexadecapolar terms). All the odd M are zero in the xy plane, and only $|0\rangle \rightarrow |-2\rangle$ ($M = -2$) and $|2\rangle \rightarrow |-2\rangle$ ($M = -4$) remain, giving an angular distribution in the xy plane $2\alpha^2 (U_{0,-2})^2 + 2\beta^2 (U_{2,-2})^2$. The relative strengths of $U_{0,-2}(\hat{x}, \hat{y}, 0) = \frac{\sqrt{3}}{2} Q_{20} \hat{x}\hat{y}$ and $U_{2,-2}(\hat{x}, \hat{y}, 0) = \frac{35}{2} A_4 \hat{x}\hat{y}(\hat{x}^2 - \hat{y}^2)$ reflect the amount of $3z^2 - r^2$ and $x^2 - y^2$ character in the ground state, respectively. Note that in the quadrupolar region, we have a simple scaling of the $\hat{x}\hat{y}$ dependence [see Fig. 2(a)]. The advantage of using hexadecapolar excitations [see Fig. 2(b)], is the clear change in angular dependence from a four-lobed to an eight-lobed shape as a function of α.

V. SUMMARY

The nonresonant inelastic x-ray scattering for local d–d transitions has been analyzed. The strong sensitivity of the angular dependence on the detailed nature of the ground state in combination with the experimental degrees of freedom (scattering angle, incoming energy) and the possible high resolution make nonresonant IXS a powerful tool to study crystal-field and orbital excitations. Future theoretical work should include an analysis for the rare-earths.

*Part of this work was done during MvV's stay at the European Synchrotron Radiation Facility.

[1] For a review, see, A. Kotani and S. Shin, Rev. Mod. Phys. **73**, 203 (2001).

[2] S. M. Butorin, J. H. Guo, M. Magnuson, P. Kuiper, and J. Nordgren, Phys. Rev. B **54**, 4405 (1996); P. Kuiper, J. H. Guo, C. Sathe, L. C. Duda, J. Nordgren, J. J. M. Pothuizen, F. M. F. de Groot, and G. A. Sawatzky, Phys. Rev. Lett. **80**, 5204 (1998); G. Ghiringhelli, N. B. Brookes, E. Annese, H. Berger, C. Dallera, M. Grioni, L. Perfetti, A. Tagliaferri, and L. Braicovich, *ibid.* **92**, 117406 (2004); S. G. Chiuzbăian, G. Ghiringhelli, C. Dallera, M. Grioni, P. Amann, X. Wang, L. Braicovich, and L. Patthey, *ibid.* **95**, 197402 (2005).

[3] M. van Veenendaal, Phys. Rev. Lett. **96**, 117404 (2006).

[4] See, e.g., M. Z. Hasan, E. D. Isaacs, Z. X. Shen, L. L. Miller, K Tsutsui, T. Tohyana, and S. Maekawa, Science **288**, 1811 (2000); Y. J. Kim, J. P. Hill, C. A. Burns, S. Wakimoto, R. J. Birgeneau, D. Casa, T. Gog, and C. T. Venkataraman, Phys. Rev. Lett. **89**, 177003 (2002).

[5] J. van den Brink and M. van Veenendaal, Europhys. Lett. **73**, 121 (2006).

[6] B. C. Larson, J. Z. Tischler, W. Ku, C. C. Lee, O. D. Restrepo, A. G. Eguiluz, P. Zschack, and K. D. Finkelstein, Phys. Rev. Lett. **99**, 026401 (2007).

[7] J. A. Soininen and E. L. Shirley, Phys. Rev. B **61**, 16423 (2000).

[8] Y. Q. Cai, P. C. Chow, O. D. Restrepo, Y. Takano, K. Togano, H. Kito, H. Ishii, C. C. Chen, K. S. Liang, C. T. Chen, S. Tsuda, S. Shin, C. C. Kao, W. Ku, and A. G. Eguiluz, Phys. Rev. Lett. **97**, 176402 (2006).

[9] I. G. Gurtubay, J. M. Pitarke, W. Ku, A. G. Eguiluz, B. C. Larson, J. Tischler, P. Zschack, and K. D. Finkelstein, Phys. Rev. B **72**, 125117 (2005).

[10] S. Galambosi, J. A. Soininen, K. Hämäläinen, E. L. Shirley, and C.-C. Kao, Phys. Rev. B **64**, 024102 (2001).

[11] K. Hämäläinen, S. Galambosi, J. A. Soininen, E. L. Shirley, J. P. Rueff, and A. Shukla, Phys. Rev. B **65**, 155111 (2002).

[12] J. A. Soininen, A. L. Ankudinov, and J. J. Rehr, Phys. Rev. B **72**, 045136 (2005).

[13] H. Sternemann, J. A. Soininen, C. Sternemann, K. Hamalainen, and M. Tolan, Phys. Rev. B **75**, 075118 (2007).

[14] M. W. Haverkort, A. Tanaka, L. H. Tjeng, and G. A. Sawatzky, Phys. Rev. Lett. **99**, 257401 (2007).

[15] See, e.g., M. B. Salamon and M. Jaime, Rev. Mod. Phys. **73**, 583 (2001).

[16] D. J. Huang, H.-J. Lin, J. Okamoto, K. S. Chao, H.-T. Jeng, G. Y. Guo, C.-H. Hsu, C.-M. Huang, D. C. Ling, W. B. Wu, C. S. Yang, and C. T. Chen, Phys. Rev. Lett. **92**, 087202 (2004).